Prediction and control of subsurface hooks in continuous-cast ultra-low-carbon steel slabs

Go-Gi Lee [a),*], Ho-Jung Shin [b)], Seon-Hyo Kim [a)], Sung-Kwang Kim [c)], Wung-Yuel Choi [c)] and Brian G. Thomas [d)]

[a)] Department of Materials Science and Engineering, Pohang University of Science and Technology, South Korea

[b)] Steelmaking Research Group, POSCO Technical Research Laboratories, South Korea

[c)] Technology Development Group, POSCO Steelmaking Department, Gwangyang Works, South Korea

[d)] Department of Mechanical Science and Engineering, University of Illinois at Urbana-Champaign, USA

[*] Corresponding author. Tel.: +82-54-279-2815; fax: +82-54-279-2399. *E-mail address:* yikoki@postech.ac.kr (Go-Gi Lee)

Abstract

Subsurface hook formation during initial solidification in the continuous casting mold degrades the quality of steel slabs owing to the associated entrapment of argon bubbles and non-metallic inclusions. To minimize hook depth and to improve slab quality, extensive plant experiments were performed and analyzed to quantify the effect of casting parameters on hook characteristics using the #2-1 caster at POSCO Gwangyang Works, South Korea. The results reveal that meniscus heat flux plays an important role in controlling hook characteristics. Hook depth correlates with oscillation mark depth, hook shell thickness, and hook length. Based on regression analysis, this paper proposes an equation to predict hook depth in ultra-low carbon steels as a function of casting speed, superheat, oscillation frequency, surface level fluctuations, and mold flux properties. Use of this quantitative equation enables improved control of subsurface quality in the continuous casting of steel slabs.

Key words: Continuous casting; Subsurface quality; Hook; Solidification microstructure; oscillation marks; Ultra-low-carbon steel

1. Introduction

Periodic transverse depressions called “oscillation marks” (OMs) are observed on the surface of steel slabs manufactured by continuous casting processes[1-3]. Hooks are another distinctive sub-surface microstructural feature, and form at the meniscus during oscillation. They lead to surface defects such as slivers and blisters in the final rolled sheet product[4, 5]. In extreme cases, the entire slab surface must be ground or “scarfed” to remove all traces of the hook microstructure, resulting in higher cost and productivity loss[6].

Many previous studies of slab quality have focused on the influences of operating parameters on oscillation marks[4, 5, 7-11] and subsurface hooks[12-16]. Ultra-low-carbon (ULC) steel grades (C≤0.01wt%) are particularly prone to hook formation as shown in Fig.1[17, 18], perhaps owing to higher liquidus temperature and thinner mushy zone[13] compared to other steel grades. These steels are designed for high ductility applications such as automobile exterior panels. Therefore, high surface slab quality is important in ULC steels. To minimize the depth of OMs and hooks and to increase slab quality, several different practices have been proposed and implemented in the industry. These include the use of mold powder with higher surface tension, higher viscosity and lower solidification temperature[19], triangular mold oscillation[20], changing the mold material for low thermal conductivity[12], and applying electro-magnetic fields for initial solidification control[21, 22].

Hooks and OMs form due to many interdependent, transient phenomena that occur simultaneously during initial solidification near the meniscus. Several different mechanisms have been proposed in previous literature. J. Sengupta et al.[23, 24] have recently suggested a new mechanism for hook and OM formation, which is illustrated in Fig.2. Hooks form in ULC steel by periodic meniscus solidification and subsequent liquid

steel overflow and OMs form by normal steel shell growth before and after the overflow. This mechanism was based on a careful analysis of numerous specially-etched samples from ULC steel slabs in controlled plant trials[6, 25] at POSCO Gwangyang Works. Furthermore, this analysis explains observations in previous literature, theoretical modeling results[23], and is supported by microstructural evidence obtained using[24] both optical microscopy and microanalysis techniques.

This present study was conducted to quantify the effect of casting conditions on OM and hook characteristics in ULC steels. Slab samples were collected during plant experiments at POSCO Gwangyang Works while controlling and measuring several operating parameters. OM and hook characteristics were measured from sections of the slab samples and correlated with operating conditions. The results obtained from these different experiments suggest practical insights to decrease hooks and their associated surface defects by controlling the phenomena that cause them in the meniscus region for ULC steels.

2. Experimental

Four separate campaigns of plant experiments and laboratory analyses were performed from 2002 to 2005. Samples of ULC steel slabs were obtained from plant experiments performed on the #2-1 conventional vertical bending slab caster at POSCO Gwangyang Works, South Korea, which features a conventional parallel-mold with 230mm thickness, standard two-port submerged entry nozzle (SEN), slide-gate flow control with argon gas, non-sinusoidal hydraulic mold oscillator and electromagnetic brake ruler system. The composition of the ULC steel grade is given in Table 1.

During the 2002 tests, two plant trial sets were performed to investigate the effect of operating parameters on OM depth and hook characteristics. Test1 was conducted at two different casting speeds with different slab width and electro-magnetic current. Test2 was conducted by changing mold oscillation conditions such as stroke, frequency, and modification ratio under the same casting speed, slab width and electro-magnetic current.

From 2003 to 2005, plant experiments (Test3 and Test4) were conducted with various casting speeds, slab widthes, and electro-magnetic currents using a different mold powder (Powder B) after performing Test1 and Test2 (Powder A). In particular, Test4 was performed to investigate the effect of casting speed on OM and hook formation. Details of the test conditions are given in Table 2 and the powder characteristics and properties are listed in Table 3 and Table 4.

Samples (230mm wide x 20mm deep x100mm long and encompassing ~10-12 OMs) were obtained near the surface of both narrow faces (NFs) of slabs for each test, as shown in Fig.3. The left NF was analyzed ultrasonically for entrapped particles (bubbles or/and inclusions) beneath the slab surface. The right NF was analyzed metallographically to measure the OM and hook characteristics. Specifically, OM depth was measured along an 80-mm length of right NF using a laser-based profilometer along 21 different lines down the NF surface. Hook characteristics were measured at five different distances between the wide faces (WFs). Further WF slab samples were taken from Test4 conditions, and hook depths were measured from 1/4 position from the corner. Sections through each sample were cut, ground, polished to ~0.25um and then etched by a special etching method[24] for ULC steel to reveal the microstructure and hook shapes.

3. Results and discussion

Hook characteristics definitions

Hook characteristics include depth, length, angle, and shell thickness as illustrated in Fig.4. The hook depth is defined for this study as the perpendicular distance from the slab surface to furthest inner extent of the hook, because this indicates the thickness of surface layer that should be removed during scarfing process to completely eliminate hooks and their associated surface defects. Hook length is defined as the linear distance from the starting point of the line of hook origin near the OM to its end point. Hook angle is derived from the depth and length and indicates how much the hook bends away from the slab surface. Hook shell thickness is usually measured at the upper end of the OM where the hook starts, which generally represents the thicker part of the hook. The OM depth is the perpendicular distance from the deepest point of the OM valley to the

reasonably flat slab surface. The average OM and hook characteristics obtained from slab samples of the right NF are given in Table 5.

In addition, the compositions of subsurface defects observed in optical micrographs near the hook region were analyzed by energy dispersive X-ray spectroscopy (EDXS), as shown in Fig.5. The complex oxides suggest mold flux and the round bubble shows evidence of non-metallic inclusions attached to it. These results show that both non-metallic inclusions and bubbles can be entrapped on the front of the solidifying shell, or hook during initial solidification at the meniscus. This agrees with previous findings[4, 18].

OM depth correlation with hook shape

Results in Fig.6 show that deeper hooks are accompanied by deeper OMs. Thus, OM depth can be used as an approximate indicator of hook depth and slab surface quality without metallographic analysis of the slabs. Many casting conditions were varied during the plant experiments, such as casting speed, slab width, mold powder, superheat, fluid flow conditions, and oscillating practice, etc. The effects of these important casting variables will be discussed in the following sections.

Hook shell thickness correlation with hook depth

Fig.7 shows that hook depth is linearly proportional to hook shell thickness. This trend holds strongly even if conditions such as mold oscillation practice have been severely changed (Test 2). This finding is consistent with the hook formation mechanism in Fig.2, which involves meniscus freezing and subsequent liquid steel overflow suggested by J. Sengupta et al[23]. Based on this mechanism, increasing the hook shell thickness indicates that either the time for the hook growth was longer or the extent of undercooling during liquid steel overflow was more pronounced. In either case, meniscus freezing is promoted so the hook becomes both thicker and longer.

Superheat effects

The effect of superheat temperature difference on hook characteristics was evaluated as part of Test2. The superheat in this study is based on tundish temperature, which should correlate with superheat at the meniscus, if the mold flow pattern stays constant. The hook length decreases dramatically for superheats above 30ºC, as shown in Fig.8. A thinner hook shell can be expected if the solidification time at the meniscus is shorter (see previous section), or if the superheat delivery is higher. Although the study in Fig.9 was conducted to investigate frequency, the effect of superheat was so important that the results were divided up accordingly. Fig 9(a) shows that the higher superheats produce thinner hooks. Fig 9(b) shows that higher superheat produces both shorter hooks and thinner hooks. Higher superheat delivery tends to make thinner and shallower hooks. Moreover, previous works has shown that hooks near the slab corners are deeper than other regions along the mold perimeter, owing to the lower superheat, and ease of meniscus overflow there[26]. These results show that raising superheat is one of the most important methods to minimize hook formation during initial solidification.

Casting speed effects

To investigate the effect of casting speed on both OM and hook depth, two different sets of plant experiments were performed between 2002 and 2005. Firstly, three casting speeds (1.40, 1.45, and 1.70m min^{-1}) are considered with different slab width in Test1 and Test2-1. Fig.10 shows optical micrographs of subsurface hooks obtained from specially-etched samples at different casting speeds. Fig.11 shows the number of entrapped particles (bubbles and/or inclusions) per unit area in samples from the left NF slab, as shown in Fig.3(a). Increasing casting speed shows a marked decrease in surface defects, contrary to expectations related to surface level fluctuation effects. These results suggest that the higher superheat found at higher casting speed is responsible for lowering hook depth and their associated surface defects.

Another set of plant experiments (Test3 and Test4) involved more systematic measurements to quantify the effect of various casting speeds and slab widths on both OM and hook depth. Firstly, increasing casting speed is known to cause a significant increase in heat extraction at the meniscus region[27], resulting in higher heat flux, as shown in Fig.12. Mean heat flux is defined as the total heat removed by the cooling water per unit area of strand surface, which is based on the measured temperature difference of the cooling water between inlet and outlet. Increasing meniscus heat flux would be expected to make hooks more severe. However, Huang and Thomas[28] noted the opposing effect that increasing the casting speed increases the local superheat delivered at the solidification front, so discourages meniscus freezing. This latter effect seems to be more important, according to the results in Figs. 13 and 14 of the current work.

Fig.13 shows that both OM and hook depths are clearly decreased with increasing casting speed, as a function of oscillation conditions such as stroke and frequency. For this analysis, 9 oscillation tests (Test2-2 ~ Test2-10) were excluded from these results because casting speed was not dependent on oscillation conditions. In addition, hook depth on the WF at 1/4 position from the corner was examined with different casting speed, as shown in Fig.14. These results again confirm that OM and hook depth decrease with increasing casting speed and the trend of decreasing hook depth with casting speed agrees with the results measured by Awajiya et al[29]. Hence, increasing casting speed, which increases flow rate of molten steel from the SEN, is expected to carry more heat to retard the initial solidification at the meniscus.

In summary, the results from several sets of tests conducted over several years show that increasing casting speed helps to increase heat delivery to the meniscus and to minimize hook and OM depth and their accompanying surface defects.

Mold powder effects

Fig.6 and 13 also show that powder properties greatly affect OM and hook depth. In this case, powder B with a lower solidification temperature and viscosity produces significantly less OM and hook depth. This effect agrees with Bommaraju et al.[19] which have been reported that mold powder with a lower solidification temperature, has shallower OM depth. This might be due to smaller slag rim solidified on the mold wall. The lower viscosity of the mold powder allows easier steel overflow at the meniscus after it freezes during hook formation. This agrees with the mechanism which was proposed by Hill et al.[30] but not with that of Kobayashi and Maruhashi[31]. Thus optimizing mold powder properties is one of the most important parameters for controlling hook depth.

Level fluctuation effects

It is well known from previous work that level fluctuations are detrimental to surface quality[32, 33]. In the current work, OM and hook depth roughly appear to decrease with decreasing level fluctuation during sampling, as shown in Fig.15. The weakness of this trend may be due to the difference of position between meniscus region and level sensor, and level fluctuations were recorded once per second using the continuous caster monitoring system, relative to ~4 mold oscillations per second. J. Sengupta et al. and Zhu[34, 35] have suggested that the thermal distortion due to a sudden level fluctuation event can cause 1) the shell tip to bend away from the mold due to sudden level drop; 2) the shell tip to further bend during the subsequent rise in liquid level. This is especially important for the shallower straight hooks. Larger level fluctuations generate deeper OMs and hooks, and also exacerbate the capture of mold slag at the solidification front. Larger level fluctuations also accompany faster, hotter steel flow to the meniscus, which is beneficial, and may explain the scatter in the trend. These results confirm the importance of controlling other casting conditions such as fluid flow in the mold, in order to control hook formation.

Mold oscillation condition effects

To investigate the effect of oscillation conditions on both OMs and hooks characteristics, Test2 plant experiments were performed holding other conditions constant, including the casting speed, slab width, mold powder (Powder A), and electro-magnetic current . Fig.16 shows the effect of oscillation conditions on OM

and hook depth from Test2. Hook depth appears to decrease with increasing oscillation frequency, but the trend with OM depth is very rough. It is difficult, however, to find a trend with stroke. Positive strip time decreases with increasing oscillation frequency, so increasing frequency shortens the solidification time. This effect helps to explain how higher frequency can produce shallower OM and hook depth with better slab surface quality. The roughness of these trends suggests that oscillation parameters are less important than the other casting conditions discussed in the previous sections.

The effects of negative and positive strip time are shown in Fig.17, divided into two groups of higher and lower superheat in Test2 plant experiments. The hook depth roughly decreases with decreasing negative strip time or decreasing positive strip time, at least for higher superheats. The importance of the superheat effect helps to explain the roughness in the trends.

Empirical equation for hook depth

From regression of the results, the following empirical equation was derived to predict the average hook depth in ultra-low carbon steel slabs from the casting conditions:

$$\text{Predicted hook depth} = 10^{-31.0874} \times Vc^{-0.61416} \times F^{-0.46481} \times T_S^{-0.18782} \times L_F^{0.041863} \times T_{Sol}^{10.692}$$

where Vc is the casting speed (m min^{-1}), F is the oscillation frequency (cycle min^{-1}), T_S is the superheat temperature difference (ºC) defined as ($T_{tundish}$-$T_{liquidus}$), L_F is the mean level fluctuation during sampling (mm) and T_{sol} is the solidification temperature of mold powder. Fig.18 compares measured hook depths with predictions using this equation.

4. Conclusions

This study presents the results of extensive parametric plant measurements of continuous-cast steel slabs to quantify the effect of process conditions on OM depth and hook characteristics. Shallower hooks correlate with shorter hooks, thinner hooks, and shallower OM depth. Hooks and their associated surface defects can be decreased by controlling the phenomena that cause them. Increasing superheat delivery to the meniscus region with increasing casting speed has a strong effect on decreasing OM and hook depths. Optimizing of mold powder properties can greatly affect hook characteristics. Level fluctuations affect hook depth. Control of casting conditions related to heat flux near the meniscus region is the key to decreasing hook depth and increasing slab quality by optimizing process conditions.

5. Acknowledgements

The authors thank the continuous casting team in Technology Development Groups of Steelmaking Department at POSCO Gwangyang Works for their efforts and cooperation during plant experiments and the Continuous Casting Consortium, the University of Illinois at Urbana-Champaign for support of this project.

6. References

1. E. Takeuchi and J. K. Brimacombe: *Metallurgical Transactions*, 1985, **16B**, 605-625.
2. E. Takeuchi and J. K. Brimacombe: *Metallurgical Transactions*, 1984, **15B**, 493-509.
3. J. K. Brimacombe and K. Sorimachi: *Metallurgical Transactions*, 1977, **8B,**, 489-505.
4. J. -P. Birat, M. Larrecq, J. -Y. Lamant, J. Petegnief, and K. T. Muller: Steelmaking Conference Proceedings, 'The Continuous Casting Mold: A Basic Tool for Surface Quality and Strand Productivity′, 1991, 74, 39-50.
5. T. Emi, H. Nakato, Y. Iida, K. Emoto, R. Tachibana, T. Imai, and H. Bana: Proc. Nat. Open Hearth and Basic Oxygen Steel Conf., 'Influence of Physical and Chemical Properties of Mold Powders on the Solidification and Occurrence of Surface Defects of Strand Cast Slabs′, 1978, 61, 350-361.

6. H.-J. Shin, B. G. Thomas, G.-G. Lee, J.-M. Park, C.-H. Lee, and S.-H. Kim: MS&T 2004, 'Analysis of Hook Formation Mechanism in Ultra Low Carbon Steel using CON1D Heat Flow Solidification Model′, New Orleans, LA, 2004, 11-26.
7. M. M. Wolf: Steelmaking Conference Proceedings, 'Mold Oscillation Guidelines′, 1991, 74, 51-71.
8. R. V. Mahapatra, J. K. Brimacombe, and I. V. Samarasekera: *Metallurgical Transactions B*, 1991, **22B**, 875-888.
9. S. Harada, S. Tanaka, H. Misumi, S. Mizoguchi, and J. Horiguchi: *ISIJ International*, 1990, **30**, 310-316.
10. A. W. Cramb and F. J. Mannion: Steelmaking Conference Proceedings, 'The Measurement of Meniscus Marks at Bethlehem Steel's Burns Harbor Slab Caster′, 1985, 68, 349-359.
11. H. Nakato, S. Matsumura, Y. Habu, H. Oka, and T. Ueda: *Tetsu-to-Hagane*, 1983, **69**, 248-253.
12. A. Yamauchi, S. Itoyama, Y. Kishimoto, and T. Watanabe: *ISIJ international*, 2002, **42**, 1094-1102.
13. H. Yamamura, Y. Mizukami, and K. Misawa: *ISIJ International*, 1996, **Supplement**, S223-226.
14. M. M. Wolf: 'Solidification Control in Continuous Casting Molds', in 'Solidification Processing 1987', (ed. edn, 182-186; 1987, Sheffield, United Kingdom, The Institute of Metals.
15. H. Nakato, T. Nozaki, Y. Habu, H. Oka, T. Ueda, Y. Kitano, and T. Koshikawa: Steelmaking Conference Proceedings, 'Improvement of Surface Quality of Continuous Cast Slabs by High Frequency Mold Oscillation′, 1985, 68, 361-365.
16. M. M. Wolf and W. Kurz: 'Solidification of Steel in Continuous Casting Molds', in 'Solidification and Casting of Metals', (ed. edn, 287-294; 1977, Sheffield, United Kingdom, The Metals Society.
17. M. Suzuki: *CAMP-ISIJ*, 1998, **11**, 42-44.
18. Y. Kitano, K. Kariya, R. Asaho, A. Yamauchi, and S. Itoyama: *Testsu-to-Hagane*, 1994, **80**, T165-168.
19. R. Bommaraju, T. Jackson, J. Lucas, G. Skoczylas, and B. Clark: *Iron & Steelmaker*, 1992, **19**, 21-27.
20. J. -P. Birat: *Revue de Metallurgie-CIT*, 1982, **79**, 603-616.
21. M. Tani, T. Toh, H. Harada, K. Fujisaki, E. Anzai, and T. Matsumiya: *CAMP-ISIJ*, 2002, **15**, 831-834.
22. T. Tho, E. Takeuchi, M. Hojo, H. Kawai, and S. Matsumura: *ISIJ International*, 1997, **37**, 1112-1119.
23. J. Sengupta, B. G. Thomas, H. J. Shin, G. G. Lee, and S. H. Kim: *Metallurgical and Materials Transactions A*, 2006, **37A**, 1597-1611.
24. J. Sengupta, H.-J. Shin, B. G. Thomas, and S. H. Kim: *Acta materialia*, 2006, **54**, 1165-1173.
25. H. -J. Shin, G. -G. Lee, W. -Y. Choi, S. -M. Kang, J. -H. Park, S. -H. Kim, and B. G. Thomas: AISTech 2004, 'Effect of Mold Oscillation on Powder Consumption and Hook Formation in Ultra Low Carbon Steel Slabs′, Nashvillle, TN, 2004, 1, 56-69.
26. G. G. Lee, B. G. Thomas, S. H. Kim, H. J. Shin, S. K. Baek, C. H. Choi, D. S. Kim, and S. J. Yu: *Acta Materialia*, 2007, **55**, 6705-6712.
27. R. B.Mahapatra, J. K. Brimacombe, and I. V. Samarasekera: *Metallurgical Transactions B*, 1991, **22**, 875-888.
28. X. Huang and B. G. Thomas: *Canadian Metallurgical Quarterly*, 1998, **37**, 197-212.
29. Y. Awajiya, J. Kubota, and S. Takeuchi: AISTech 2005, 'Inclusion Entrapment Location in Solidified Shell of Ultra Low Carbon Steel Slab′, 2005, 2, 65-74.
30. J. M. Hill, Y. H. Wu, and B. Wiwatanapataphee: *Journal of Engineering Mathematics*, 1999, **36**, 311-326.
31. Y. Kobayashi and S. Maruhashi: 4th Japan-CSSR Seminar, Ostrava, 1983, 249.
32. J. Kubota, K. Okimoto, M. Suzuki, A. Shirayama, and T. Masaoka: ISC. 6th Int. Iron and Steel Congr., Nagoya, Japan, 1990, 3, 356-363.
33. Y. Sasabe, S. Kubota, A. Koyama, and H. Miki: *ISIJ*, 1990, **30**, 136-141.
34. B. G. Thomas and H. Zhu: JIM / TMS Solidification Science and Processing Conference, 'Thermal Distortion of Solidifying Shell near Meniscus in Continuous Casting of Steel′, Honolulu, HI, 1995, 197-208.

35. J. Sengupta and B. G. Thomas: Modeling of Casting, Welding and Advanced Solidification Processes - XI, 'Effect of a Sudden Level Fluctuation on Hook Formation During Continuous Casting of Ultra-low Carbon Steel Slabs′, Opio, France, 2006, 727-236.

Table 1 Composition of ultra-low carbon steel tested (wt %)

C	Mn	Si	P	S	Cu	Ti	Al
0.002 ~ 0.005	0.05~0.15	≤ 0.005	≤ 0.015	≤ 0.010	~ 0.01	~0.050	~ 0.05

Table 2 Test conditions from controlled plant experiments

Test No.	Slab width (mm)	Casting speed (m min^{-1})	Electro-magnetic current (A)	Tundish temp. (˚C)	Liquidus temp. (˚C)	Level fluctuation during sampling (mm)	Oscillation stroke (mm)	Oscillation frequency (cycle min^{-1})	Non-sinusoidal mold oscillation ratio (%)	Negative strip time (s)	Positive strip time (s)
Test1-1	980	1.40	304.0	1559	1532.1	0.65	6.37	155	24	0.110	0.277
Test1-2	1050	1.70	405.0	1561	1532.1	1.05	6.82	181.3	24	0.095	0.236
Test2-1	1300	1.464	300.8	1566	1534.9	1.06	6.44	159.3	24	0.107	0.269
Test2-2	1300	1.457	300.6	1563	1534.9	1.78	5.00	145.7	0	0.115	0.296
Test2-3	1300	1.468	300.0	1571	1534.9	0.82	5.00	176.2	12	0.100	0.241
Test2-4	1300	1.496	297.4	1571	1534.2	0.94	5.00	209.4	24	0.081	0.205
Test2-5	1300	1.501	299.8	1555	1534.9	0.61	6.00	125.1	12	0.127	0.353
Test2-6	1300	1.468	300.2	1573	1534.2	0.65	6.00	146.8	24	0.110	0.299
Test2-7	1300	1.490	301.4	1566	1534.9	1.62	6.00	173.9	0	0.121	0.224
Test2-8	1300	1.487	302.0	1571	1534.9	0.96	7.00	106.2	24	0.139	0.426
Test2-9	1300	1.466	303.0	1559	1534.9	1.03	7.00	125.6	0	0.154	0.324
Test2-10	1300	1.493	300.4	1559	1534.9	0.76	7.00	149.3	12	0.126	0.276
Test3-1	1300	1.747	313.4	1560	1534.9	0.66	7.49	186.8	18	0.100	0.221
Test3-2	1300	1.418	234.2	1564	1535.0	0.47	6.84	154.7	18	0.118	0.269
Test3-3	1300	1.210	0.0	1564	1535.0	0.46	6.42	134.5	18	0.134	0.312
Test3-4	1300	1.474	277.0	1571	1535.0	0.71	6.95	160.2	18	0.115	0.260
Test3-5	1300	1.460	2.0	1567	1535.0	0.62	6.92	158.9	18	0.116	0.262
Test4-1	950	1.803	456.8	1559	1533.5	0.54	6.30	192.3	19	0.092	0.220
Test4-2	950	1.805	457.0	1559	1533.5	0.37	6.30	192.4	19	0.092	0.220
Test4-3	950	1.793	307.6	1559	1533.5	0.12	6.29	191.3	19	0.092	0.221
Test4-4	1300	1.692	232.0	1564	1534.9	1.99	6.19	181.5	19	0.092	0.234
Test4-5	1300	1.396	232.2	1564	1534.9	0.72	5.90	152.6	19	0.114	0.279
Test4-6	1300	1.684	232.2	1565	1534.9	0.94	6.18	180.7	19	0.097	0.235
Test4-7	1300	1.689	235.8	1564	1534.9	0.62	6.19	181.2	19	0.097	0.234
Test4-8	1440	1.506	190.4	1562	1534.9	0.55	6.01	163.4	19	0.107	0.261
Test4-9	1440	1.509	236.0	1562	1534.9	1.36	6.01	163.6	19	0.107	0.260
Test4-10	1570	1.373	139.8	1566	1534.6	0.80	5.87	150.4	19	0.115	0.284
Test4-11	1570	1.374	140.0	1565	1534.2	1.28	5.87	150.5	19	0.115	0.283
Test4-12	1570	0.990	0.0	1568	1534.2	3.07	5.49	113.0	19	0.152	0.379
Test4-13	1570	0.835	0.0	1570	1534.2	1.45	5.34	97.9	19	0.175	0.438

Table 3 Mold powder compositions (wt %)

	Basicity	SiO_2	CaO	MgO	Al_2O_3	TiO_2	Fe_2O_3	MnO_2	P_2O_5	Na_2O	K_2O	F	B_2O_3	Li_2O
Powder A (Test 1 and 2)	1.1	36.33	39.80	0.84	5.97	0.18	0.34	0.03	0.03	3.43	0.11	6.72	0.0	0.35
Powder B (Test 3 and 4)	1.0	37.77	37.88	1.98	4.99	0.03	0.31	0.04	0.01	3.75	0.11	7.22	1.20	0.90

Table 4 Mold powder properties

	Bulk density ($g\ ml^{-1}$)	Solidification temperature (˚C)	Softening temperature (˚C)	Melting temperature (˚C)	Viscosity (poise) at 1300˚C
Powder A (Test 1 and 2)	0.82	1150	1170	1180	3.21
Powder B (Test 3 and 4)	0.85	1100	1150	1150	2.62

Table 5 Mean value of hook characteristics and OM depth

Test No.	Measured hook depth (mm)	Measured hook length (mm)	Measured hook angle (degree)	Measured hook shell thickness (mm)	Measured OM depth (mm)
Test1-1	1.87	6.37	18.5	-	0.440
Test1-2	1.2	2.81	30.0	-	0.286
Test2-1	1.68	2.16	34.3	0.71	0.246
Test2-2	2.16	4.72	19.8	0.86	0.393
Test2-3	1.39	2.16	27.6	0.66	0.309
Test2-4	1.54	2.41	29.7	0.65	0.292
Test2-5	1.72	3.34	23.1	0.76	0.353
Test2-6	1.69	2.75	28.7	0.7	0.343
Test2-7	1.59	2.77	27.5	0.62	0.258
Test2-8	1.89	3.08	29.7	0.78	0.308
Test2-9	2.32	4.87	21.6	0.92	0.338
Test2-10	1.94	4.58	20.2	0.78	0.331
Test3-1	1.1	2.0	27.0	0.46	0.251
Test3-2	1.22	1.77	30.9	0.52	0.328
Test3-3	1.3	1.63	34.6	0.60	0.280
Test3-4	1.18	1.83	26.1	0.56	0.313
Test3-5	1.06	1.65	28.0	0.46	0.272
Test4-1	0.83	-	-	0.45	0.225
Test4-2	0.83	-	-	0.41	0.214
Test4-3	0.73	-	-	0.38	0.199
Test4-4	0.77	-	-	0.47	0.192
Test4-5	1.11	-	-	0.51	0.302
Test4-6	1.06	-	-	0.53	0.236
Test4-7	0.96	-	-	0.47	0.277
Test4-8	1.09	-	-	0.49	-
Test4-9	1.03	-	-	0.46	-
Test4-10	1.12	-	-	0.57	0.310
Test4-11	1.05	-	-	0.53	0.304
Test4-12	1.79	-	-	0.73	0.495
Test4-13	1.62	-	-	0.71	0.566

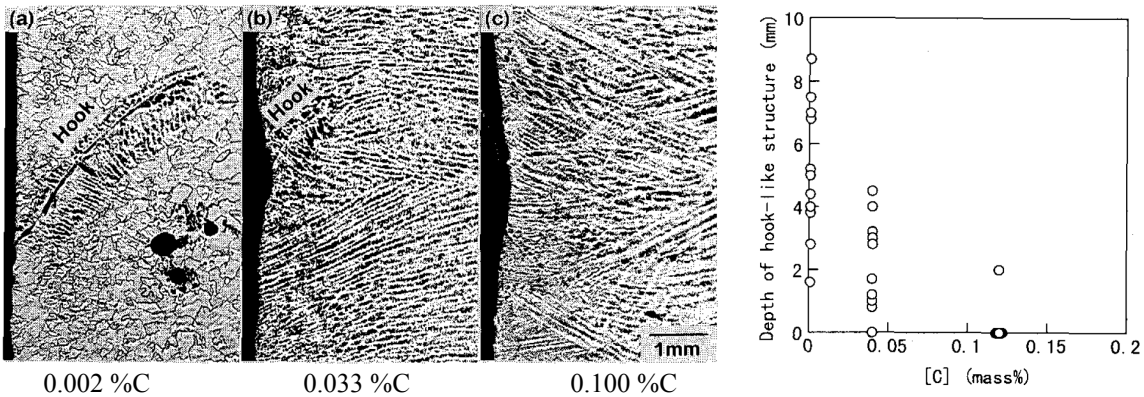

0.002 %C 0.033 %C 0.100 %C

Fig. 1. Effect of steel carbon content on hook depth [17, 18)]

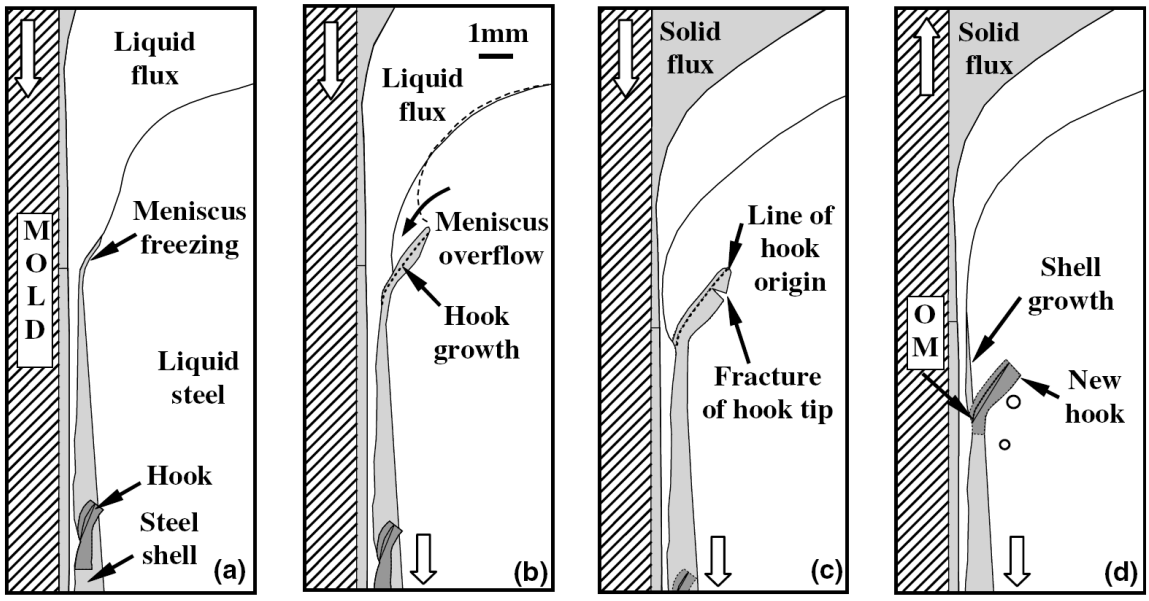

(a) (b) (c) (d)

Fig. 2. Schematic illustrating formation of curved hooks in ULC steel slabs by meniscus solidification and subsequent liquid steel overflow [23, 24)]

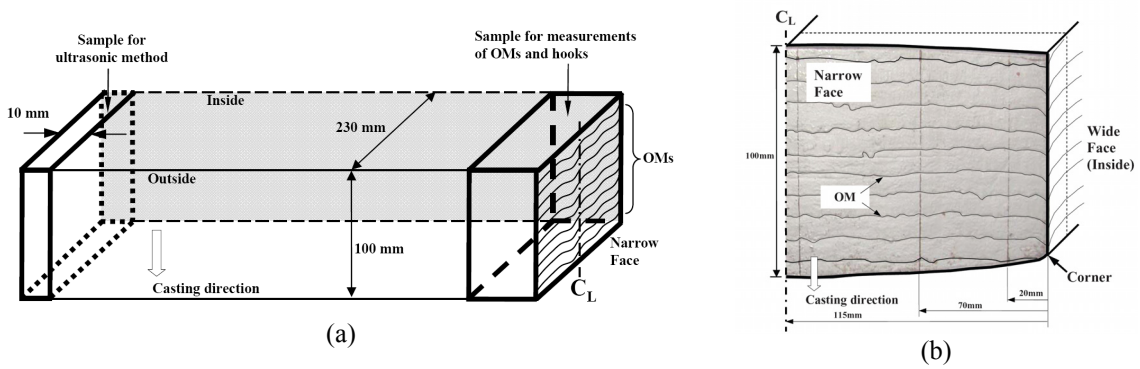

Fig. 3. Schematic showing sample locations for (a) both NFs and (b) measurements of OMs and hooks on the right NF

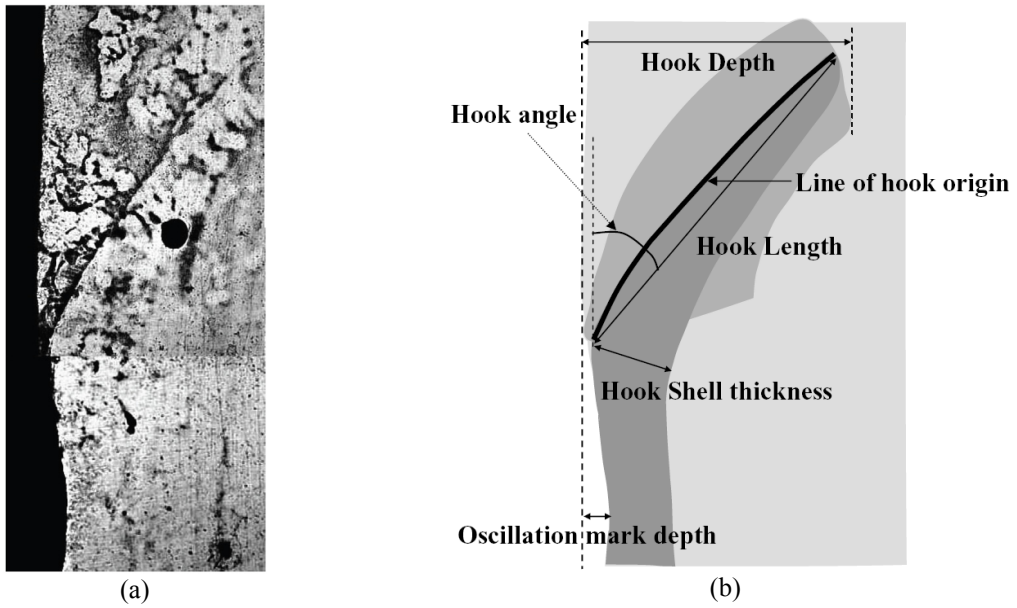

Fig. 4. (a) Typical shape of curved hook with entrapped bubble and (b) definitions of hook characteristics

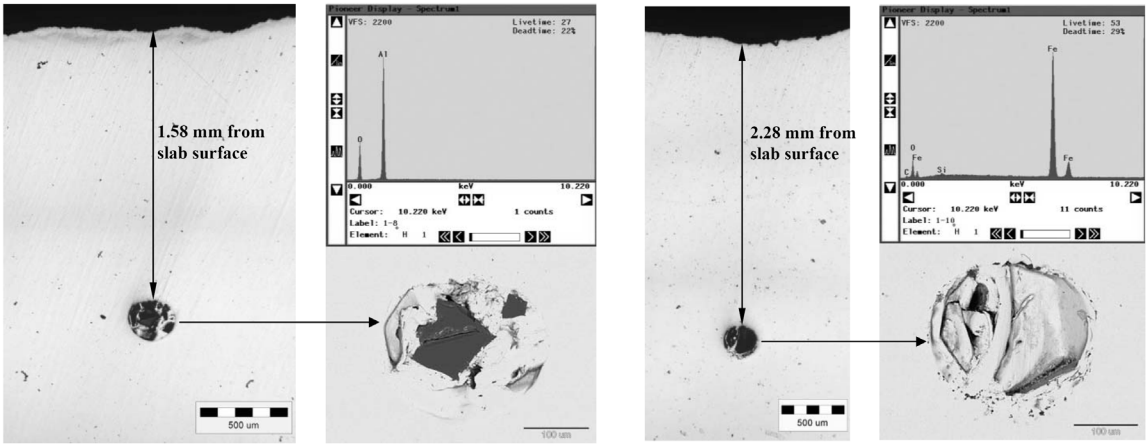

(a) (b)

Fig. 5. Optical micrographs showing entrapment of inclusions attached to round bubble beneath slab surface

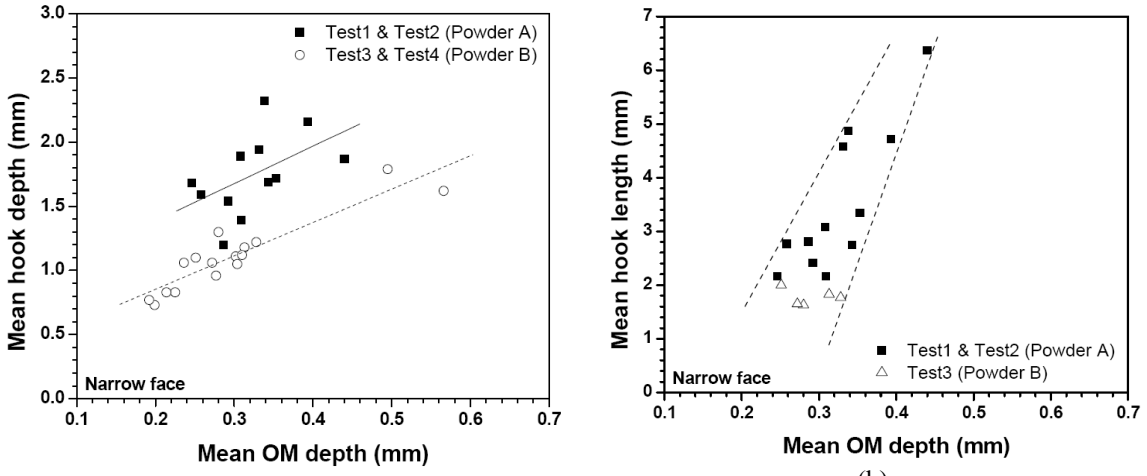

(a) (b)

Fig. 6. Relation between OM depth and hook shape: (a) depth and (b) length

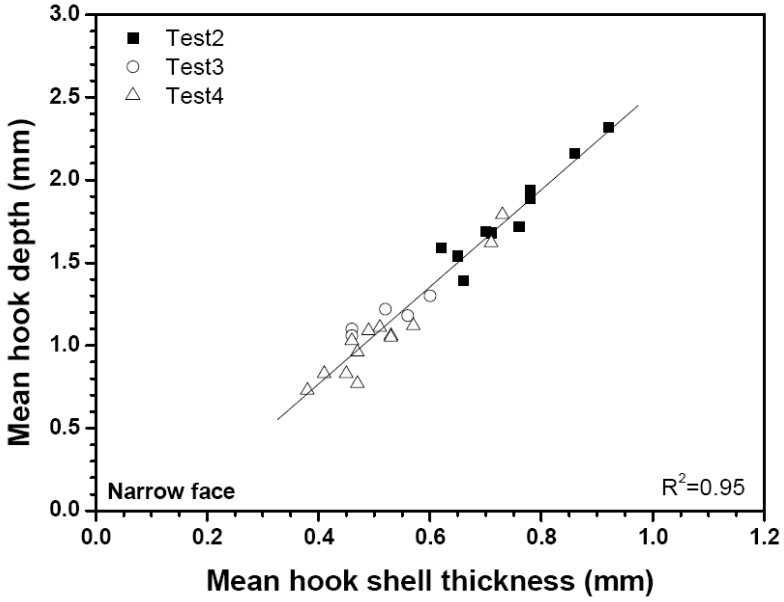

Fig. 7. Relation between hook shell thickness and depth

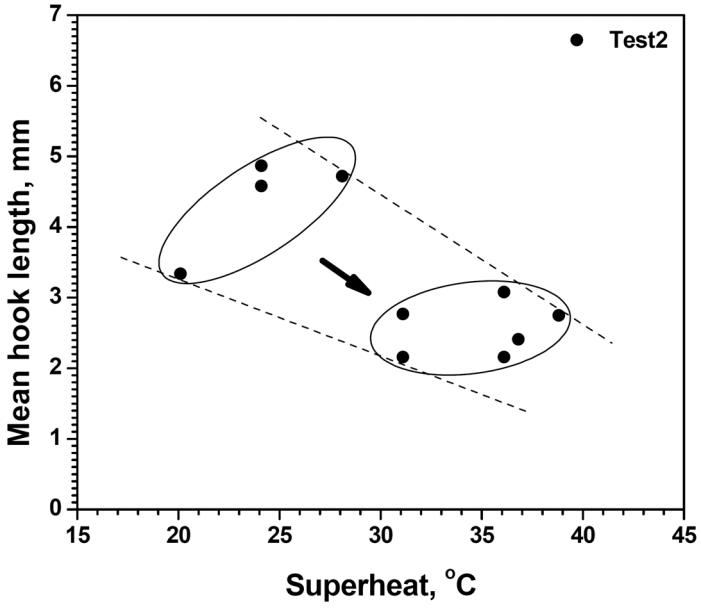

Fig. 8. Effect of superheat on hook length

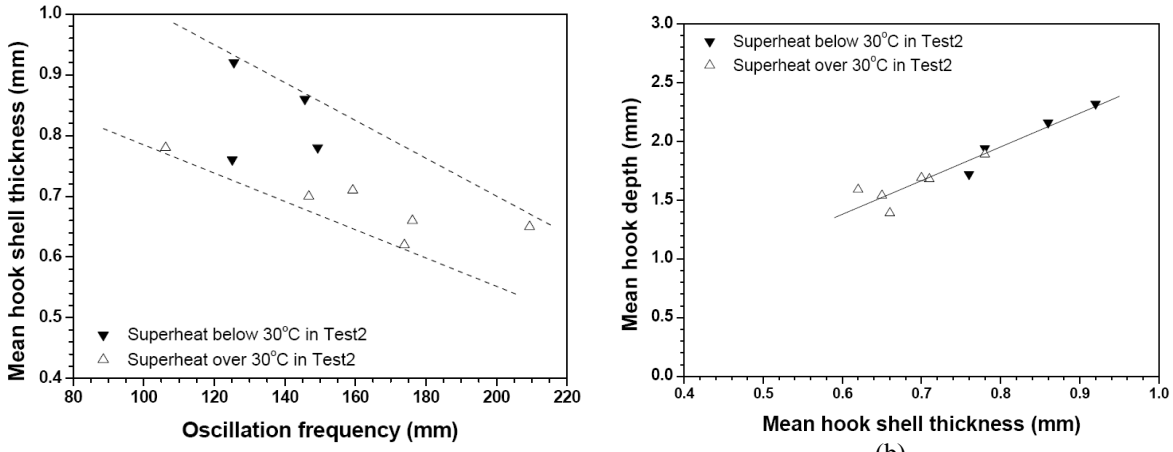

(a) (b)

Fig. 9. Relation between superheat and hook shape

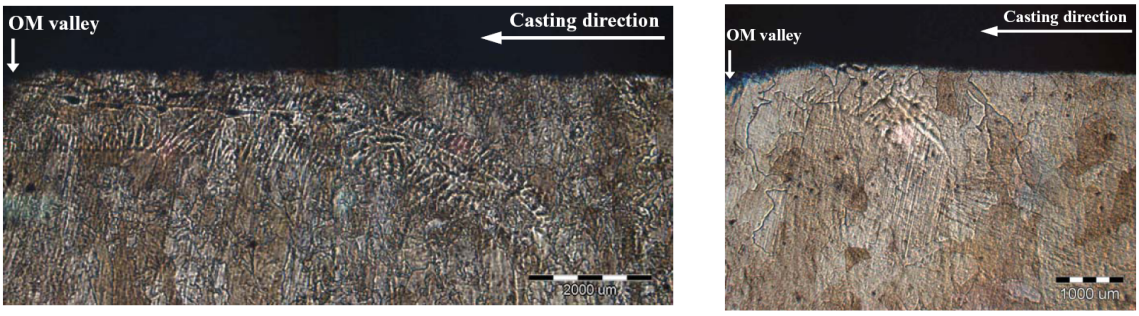

(a) (b)

Fig. 10. Optical micrographs of subsurface hook at different casting speeds; (a) 1.40m/min (b) 1.70m/min

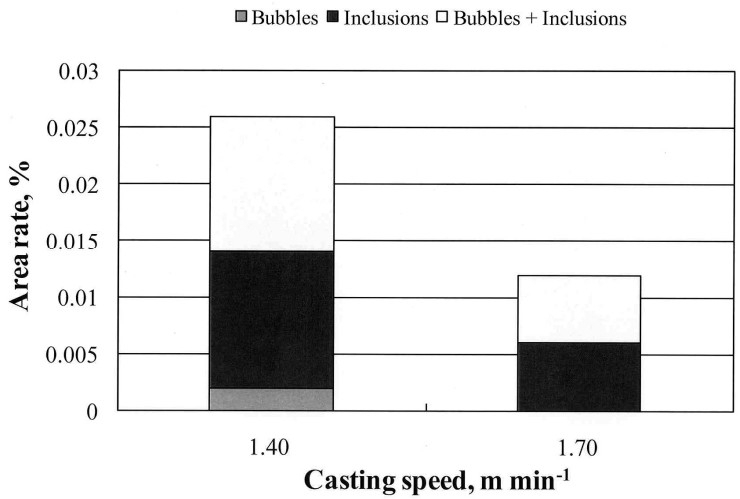

Fig. 11. Relation between casting speed and surface defects

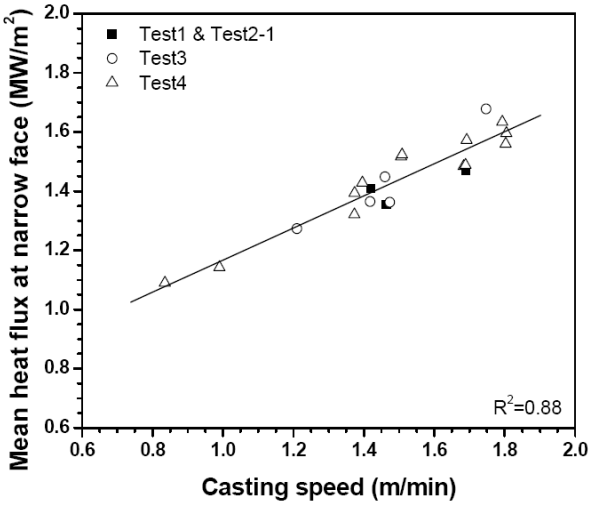

Fig. 12. Relation between casting speed and heat flux at NF

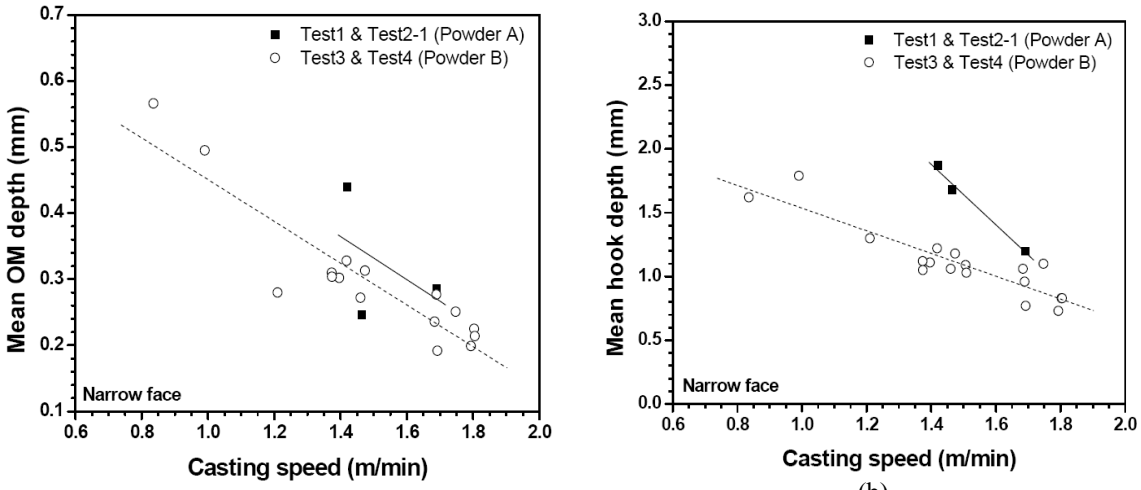

(a) (b)

Fig. 13. Effect of casting speed on (a) OM and (b) hook depth on NF

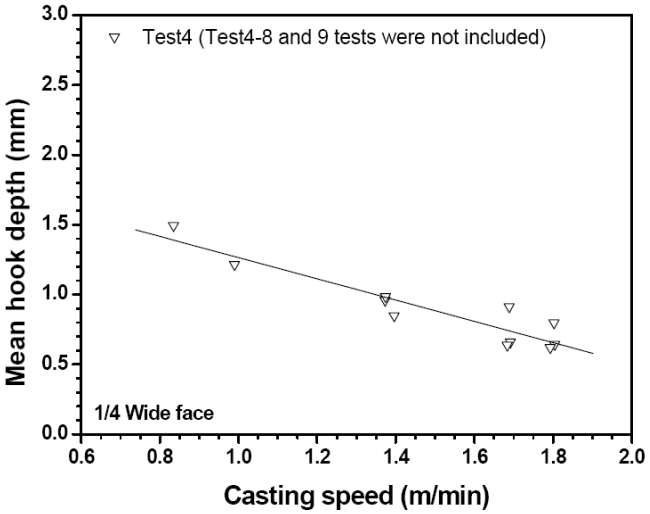

Fig. 14. Effect of casting speed on hook depth of WF

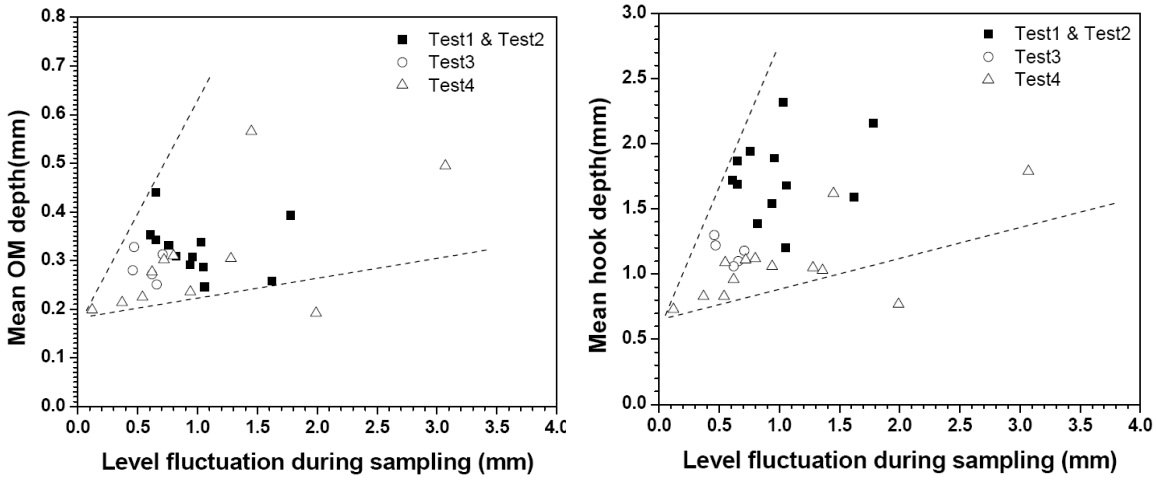

(a) (b)

Fig. 15. Effect of level fluctuation during sampling on (a) OM and (b) hook depth

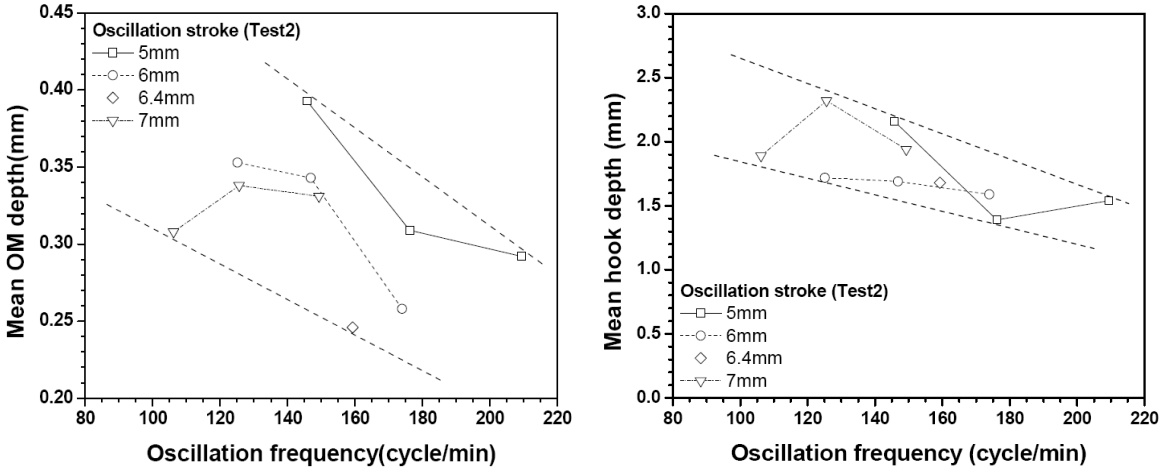

(a) (b)

Fig. 16. Effect of oscillation frequency on (a)OM and (b) hook depth

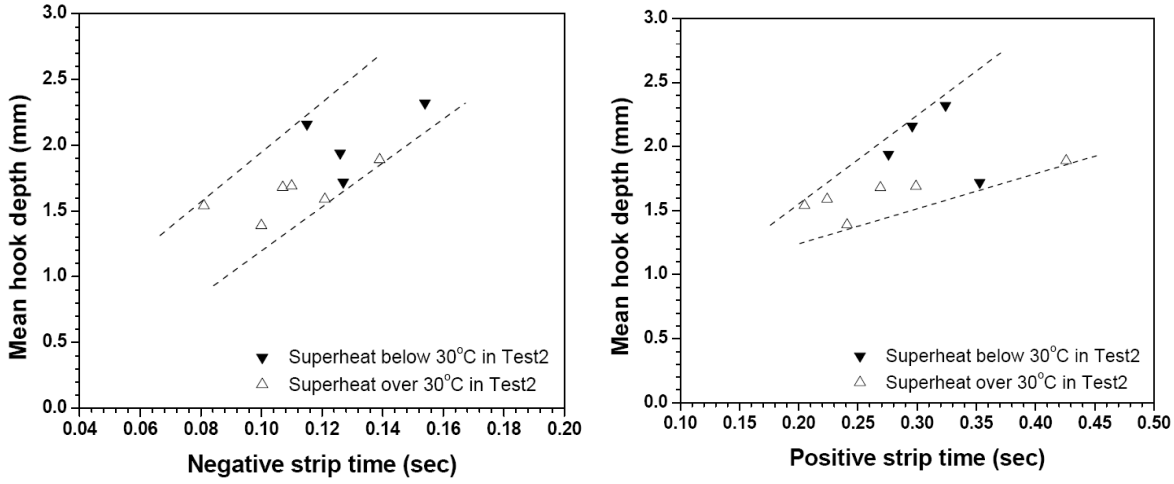

(a) (b)

Fig. 17. Effect of mold oscillation on hook depth: (a) negative strip time and (b) positive strip time

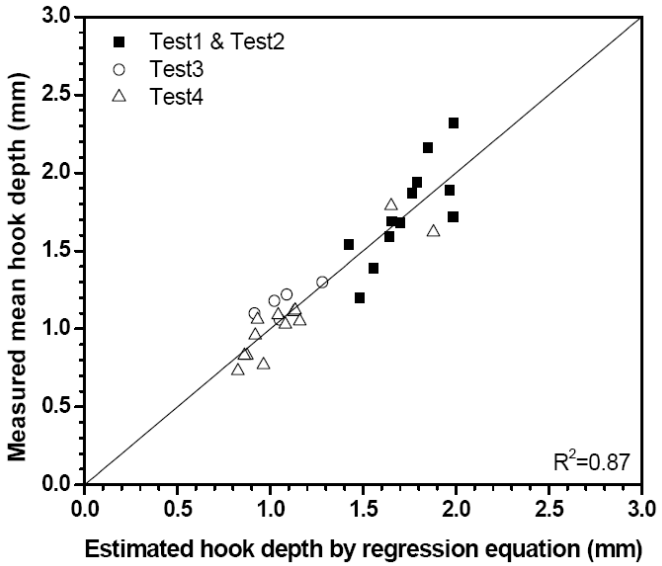

Fig. 18. Simple emirical equation with experimental results